

BRITTLE FRACTURE OF PLATES IN TENSION. STRESS FIELD NEAR THE CRACK

VIKRAM K. KINRA

Department of Mechanical Engineering, University of Colorado, Boulder, CO 80309, U.S.A.

and

CHARLES L. BOWERS

Shell Oil Company, Martinez, CA 94553, U.S.A.

(Received 14 January 1980)

Abstract—Stress waves emitted during tensile fracture of thin soda-lime glass plates have been measured using conventional strain-gage techniques. A rather novel method of obtaining a triggering signal is also described. It was found that for the case of points lying on the prospective fracture plane, where the analytical solutions are available, the theory and the experiments agree quite well. Experimental results were also obtained for points some small distance away from the crack path.

INTRODUCTION

The problem of stress waves emitted during brittle fracture has received considerable attention in recent years (see [1, 2]). Amongst the experimental contributions may be mentioned the work of Kobayashi and his co-workers (who were mainly interested in the dynamic stress intensity factor, e.g. [5]) and Kolsky and his co-workers (who measured the emitted waves at locations remote from the site of the fracture; see Refs. [3, 4]). Very little work regarding the dynamic stresses in the vicinity of the crack plane has been reported; this is the subject of the present investigation.

Another motivation for this work was provided by a recent work by Kinra and Kolsky[4], who studied fracture of glass beams in *pure* bending. An interesting observation of their work is that, contrary to expectation, the crack tip enters the *initially* compressive half of the beam without any appreciable change in crack velocity. They *conjectured*, therefore, that some sort of tensile stress field must be radiated in front of the moving tip that annihilates the initial compression. The present work sheds some light on this subject.

Single-edge-notched (SEN) plates of glass were fractured in pure tension. At first, the measurements were restricted to points lying on the prospective crack path. These were compared with the analysis of Freund[6]; the agreement was found to be remarkably good. Later, stresses at points some distance away from the crack path were also measured. These stress wave measurements contain, of necessity, reflections from the notched edge of the plate and hence are not truly "virgin" in nature. However, a large fraction of the data was collected prior to the arrival of any other boundary reflection.

THEORETICAL CONSIDERATIONS

Consider an SEN plate subjected to a remotely applied uniform tension which is increased quasi-statically until crack extension takes place (Fig. 1). The crack propagation causes a total and instantaneous relaxation of the stress ahead of the crack tip: as a result, stress waves are propagated. In the following, an expression for the stress $\sigma_{22}(x_1, 0, t)$ is derived using the results of Freund[6], who has considered the problem of a semi-infinite crack in an infinite body. A plane-strain Mode I deformation of the body is assumed. For $t < 0$, let the normal stress ahead of the crack tip be $\sigma_{22} = -p(x_1)$. The crack is at rest and occupies $x_2 = 0^+$, $x_1 < 0$. At $t = 0$ the crack begins to extend at a constant velocity v . Let σ_{22}^* be the *dynamic* component of stress at any point on the prospective fracture plane, then,

$$\sigma_{22}^*(x_1, 0, t) = \int_0^{x_1} \sigma_{22}^*(x_1 - x_0, 0, t - x_0/v) p(x_0) dx_0 \quad (1)$$

where $\sigma_{22}^*(\xi, 0, t)$ is the so-called fundamental solution, i.e. the solution to the foregoing

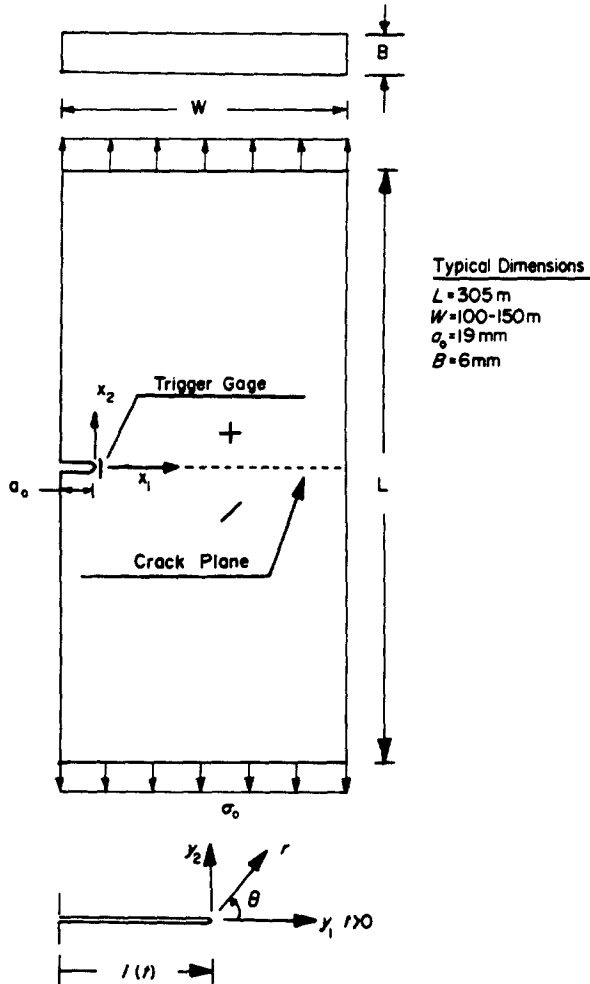


Fig. 1. Schematic of a typical specimen.

problem with $-p(x_1) = \delta(x_1)$. With $\xi = x_1 - vt$,

$$\sigma'_{22}(\xi, 0, t) = -\frac{\mu}{\pi\xi} \frac{\text{Im}[H_+(-t/\xi)]}{(d + t/\xi)}, \quad t > a_2\xi \tag{2}$$

where μ is the shear modulus, $H_+(\lambda) = -(d^{-1/2}(d-c)(\lambda + c_2)/\mu\alpha_+(\lambda))$, $\alpha_+(\lambda) = [a + \lambda(1 - a/d)]^{1/2}$, $c_2 = c/(1 - c/d)$, and a, b, c, d are respectively the slownesses of dilatational, distortional, and Rayleigh waves and the crack tip. Substituting for ξ in (2) and the resulting expression in (1) we get,

$$\sigma_{22}^*(x_1, 0, t) = -\frac{\mu}{\pi} \int_0^{vt} \frac{\text{Im}[H_+(-\gamma)]p(x_0)}{(x_1 - vt)(d + \gamma)} dx_0 \tag{3a}$$

where $\gamma = (t - x_0/v)/(x_1 - vt)$. It may be shown that $H_+(-\gamma)$ is real for $x_0 > x_{0CR} = (t - ax_1)/(d - a)$ and imaginary for $x_0 < x_{0CR}$. Making a series of appropriate substitutions, one obtains

$$\sigma_{22}^*(x_1, 0, t) = \frac{1}{\pi(x_1 d - t)^{1/2}} \int_0^{x_{0CR}} \frac{p(x_0)[x_0(d - c) - (t - cx_1)]}{(x_1 - x_0)[(t - ax_1) - x_0(d - a)]^{1/2}} dx_0 \tag{3b}$$

for $ax_1 < t < dx_1$, and $\sigma_{22}^*(x_1, 0, t) = 0$ otherwise.

In order to use this solution for the problem under consideration, a number of assumptions

have to be introduced. Typical dimensions of a specimen are shown in Fig. 1. Essentially *plane stress* conditions are obtained in the experiments. The analysis[6], however, is based on the assumption of *plane strain*. Next, in the analysis the waves traveling in the negative x_1 direction are diffracted by the traction-free crack surfaces $-\infty < x_1 < vt$, $x_2 = 0^\pm$. In the experiments, however, these waves are reflected by the "left" edge of the plate at $x_1 = -a_0$. Finally, in view of the fact that an exact solution for $-p(x_1)$ involves heavy algebra, it is assumed that $-p(x_1)$ is the same as in a centrally cracked plate, i.e. $-p(x_1) = \sigma_0/[1 - a_0^2/(x_1 + a_0)^2]^{1/2}$, $x_1 > 0$. The results of the theory and the experiment will nevertheless be compared keeping these discrepancies in mind. Substituting for $p(x_0)$ in eqn (3b) and letting $\Sigma_{22}^* = \sigma_{22}^*/\sigma_0$,

$$\Sigma_{22}^* = \frac{-1}{\pi(x_1 d - t)^{1/2}} \int_0^{x_0cr} \frac{1}{[1 - a_0^2/(x_0 + a_0)^2]^{1/2}} \frac{1}{(x_1 - x_0)} \frac{[x_0(d - c) - (t - cx_1)]}{[(t - ax_1) - x_0(d - a)]^{1/2}} dx_0.$$

Finally, the total stress is given by,

$$\Sigma_{22}^* = (\sigma_{22}/\sigma_0) = 1 + \Sigma_{22}^*. \tag{5}$$

Freund[7] observed that a discontinuity in stress is propagated with the dilatational wavefront. Using eqn (4), it can be readily shown that the strength of this discontinuity in Σ_{22} is

$$[\Sigma_{22}] = \frac{-1}{\sqrt{x_1}} \frac{(d - c)}{(c - a)} \left(\frac{a_0}{2}\right)^{1/2}.$$

Observe that this discontinuity disappears as the singularity in $p(x_1)$ near $x_1 = 0$ disappears, i.e. as $a_0 \rightarrow 0$.

EXPERIMENTAL PROCEDURES

A typical specimen and loading fixtures are shown in Figs. 1 and 2. In order to suppress bifurcation of the crack, a rather deep notch (~ 20 mm) was introduced. This was done in two

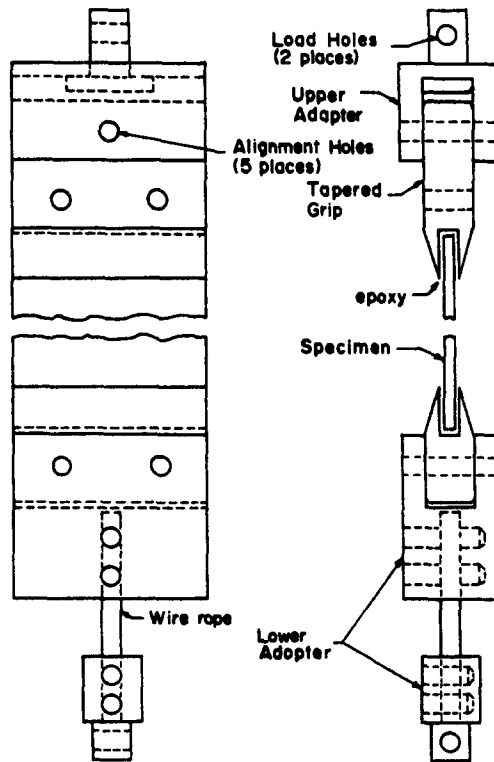


Fig. 2. Loading fixtures for the specimen.

stages. First, a diamond saw was used to cut to a depth of about 15 mm. When the early experiments were conducted with this type of notch, it was found that the crack propagates initially at some angle to the x_1 -axis. Because of strain gages mounted symmetrically on either side of the expected fracture plane, even this small deviation of the crack path could not be tolerated. Consequently, in the later experiments the second part of the notch (~ 5 mm) was cut with a very fine diamond-impregnated wire of 0.127 mm (0.005 in.) diameter. This resulted in a much smoother notch-root and consequently the crack deviated less than 1 mm of the expected crack path for the entire length of crack propagation. A soft, flexible epoxy (TRACON BC-2139) was used to bond the glass specimen to the aluminum grips. The out-of-plane bending was minimized by using a special jig during specimen preparation; the jig simulated the Instron testing machine and its use assured that the mid-plane of the specimen is aligned accurately to within ± 0.1 mm. In addition, a wire rope incorporated between the loading fixture and the Instron ensured that the bending moment transmitted to the specimen, if any, would be negligibly small.

Two different methods were employed to convert the fracture event into a triggering pulse. In the first, the crack severed a thin coat of conductive silver paint directly ahead of the crack tip; this has been described in [3, 4]. A shortcoming of this technique is that it involves an irreproducible time delay of about 10 μ sec. It was desirable to limit the triggering delay to a few microseconds and, more importantly, to make it reproducible to within 1 μ sec. To this end, a very sensitive strain gage (1000 Ω , 3.2 Gage Factor) was mounted directly ahead of the notch. When fracture occurred, the crack propagated through the middle of the strain gage; however, due to its higher ductility, the gage itself did not fracture for about 15 μ sec. Assuming that the ends of the strain gage move apart by an amount equal to the crack-opening-displacement (COD), the gage develops about 1 mV output (for the particular circuit used to energize it) in 1 μ sec. This signal was amplified 500 times and applied to a Schmitt trigger circuit whose threshold was set to about 100 mV. The output of the Schmitt trigger (24 V) was used to trigger the oscilloscopes. The time delay between the arrival of crack tip at the center of the trigger gage and the triggering of the oscilloscopes was estimated to be about 1 μ sec and was confirmed by the experiments. Micro-Measurement strain gages (ED-DY-125AC-10C, 1000 Ω , Gage Factor 3.2) were used for all measurements.

Calibration

Equation (5) is based on the assumption of constant crack velocity. It is well known that in extremely brittle materials such as glass, the crack accelerates rapidly from some initial velocity to a nearly constant terminal velocity. If the period of acceleration is small compared to the total period of observation, then the results of the experiments may be compared with eqn (5). To this end several experiments were conducted to measure the crack velocity, using a well known technique in which strands of conductive silver paint are broken by the advancing crack tip (see [10] for example). It was found that during about the first 10 mm of crack extension, the crack velocity was small and varied considerably from one test to another. However, for the subsequent motion (about 120 mm) the velocity was both reproducible and nearly constant. The results of 28 such measurements gave the average velocity $v = 1.639$ mm/ μ sec. In the following, the initial acceleration is ignored and a constant velocity crack extension is assumed. Next, some assumption has to be made regarding the initial distribution of the stress σ_{22} at $x_2 = 0$. Since the mid-section $x_2 = 0$ is only one plate width away from the loading ends, St-Venant's principle cannot be invoked to claim uniform stress distribution. Consequently, an *uncracked* specimen was fabricated out of a photo-elastic material (Columbia Resin CR-39) and was mounted in a manner identical to that used for the glass specimens. A bright field arrangement of a circular polariscope was used [8]. The specimen was loaded in simple tension and color photography was used to record the resulting fringe patterns. No color differences were detected across the entire width of the mid-section up to a load corresponding to the 2nd order fringe, which means that the variation in stress was less than 8% [8]. Finally, the out-of-plane bending was examined by mounting two strain gages facing each other—one on each face of the specimen. The maximum bending stress was found to be less than 5% of the applied tension.

Stress field on the fracture plane

The first series of tests was concerned with the measurement of surface strains at points lying on the prospective fracture plane. A typical specimen is shown in Fig. 3(b). The dynamic strain gage records are included in Fig. 3(a): here $\epsilon_{\alpha\beta}$ are the dynamic strains. Initially $\sigma_{11} = \sigma_{12} = 0$, therefore, unlike σ_{22} , no distinction need be made between the dynamic and the total stress: Let $\Sigma_{11} = \sigma_{11}/\sigma_0$ and $\Sigma_{12} = \sigma_{12}/\sigma_0$. A state of plane stress was assumed for data reduction. The experimental and the analytical results for Σ_{22} are compared in Fig. 3(c). The agreement between the theory and the experiment is considered remarkably good. The discontinuity in stress, expected at $t = 10 \mu\text{sec}$, is not seen because the time delay between the onset of fracture and triggering of the oscilloscopes was also about $10 \mu\text{sec}$. (In later experiments with smaller time-delays, it was found that a slight dip in Σ_{22} occurs at the time when the discontinuity is expected). For the trace of Σ_{11} , the data after the maximum at $t = 35 \mu\text{sec}$ is discarded because the material underlying the strain gage has been split in two. Since an expression for Σ_{11} is not available, the experiment and the theory could not be compared for this case.

An interesting feature of these results with *plates* is that the stress field propagated *ahead* of the crack is tensile in all in-plane directions. This is in marked contrast to the compressive unloading waves which are propagated in the *axial* direction when slender *rods* are fractured either in tension or in bending [3, 4]. The two, however, in no way contradict each other. The tensile cylindrical pulses propagated *ahead* of the crack attenuate rapidly due to geometric dispersion and successive reflections at the boundaries. Therefore, even though their magnitude is appreciable near the fracture plane, at rod sections several diameters away from the crack plane the magnitude becomes negligibly small. On the other hand, the compressive stress pulses propagated in the *axial direction* are essentially plane in nature and propagate without

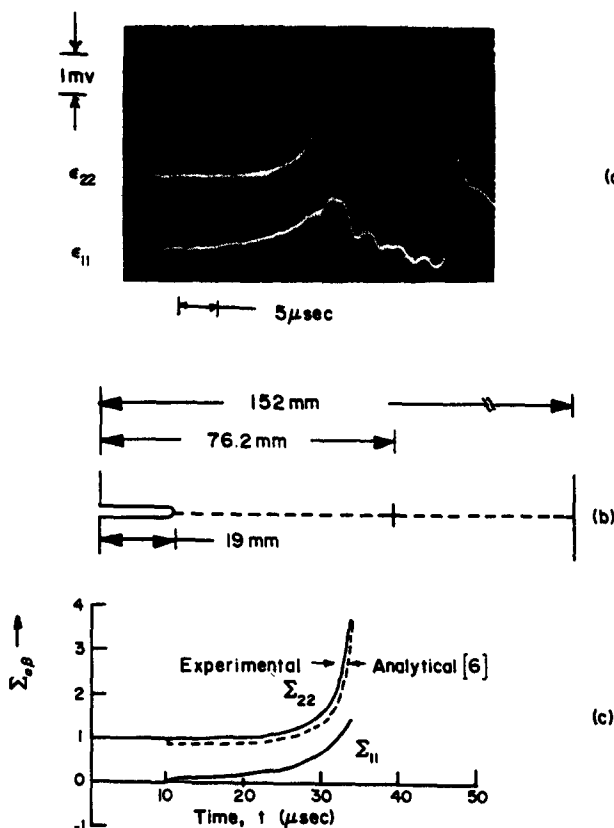


Fig. 3. (a) Dynamic strain gage records for the fracture of the specimen schematically shown in (b). (c) Comparison of analytical and experimental results.

appreciable dispersion. This accounts for the compressive nature of the longitudinal pulses in the experiments with rods [3, 4].

Stress field near the fracture plane

The next series of experiments was concerned with the measurement of stress field at points some small distance *away* from the fracture plane. For these tests, three strain gages were mounted symmetrically as shown in Fig. 4. Since the crack tip does not pass through any of the gages, some independent criterion had to be used to fix accurately the time of onset of fracture. Rice [9] has given the solution, in terms of the near-tip stress field, for steady-state crack propagation at constant velocity. We assume that when the crack tip is very near the strain gage, the actual distribution may be approximated by that of [9]. This assumption was used to locate the position of the crack tip at the instant when Σ_{22} reaches a maximum; the time of fracture initiation ($t = 0$) could then be fixed on the oscillograph traces. The results of a typical experiment are shown in Fig. 4. On the upper trace t_c and t_r denote, respectively, times corresponding to the arrival of the crack tip at $34 \mu\text{sec}$ and the first reflection from the right edge at $38.4 \mu\text{sec}$ (based on the plate wave velocity of 5460 m/sec [11], which is the appropriate velocity to be used here, since the wave has traveled several plate thicknesses). The lack of activity for the first ten microseconds corresponds to the fact that the plate wave does not arrive until $t = 10.4 \mu\text{sec}$. Even after this front arrives there is little activity in either Σ_{22} or Σ_{12} until the Rayleigh wavefront arrives at $t = 18 \mu\text{sec}$. On the other hand, Σ_{11} becomes active soon after the arrival of the plate wavefront. The trace for Σ_{11} exhibits a well defined "double-peak" behavior as the crack tip passes by the strain gage. The second peak cannot be attributed to the reflection from the right edge for the following reasons: (1) the wavefront of the right edge reflection arrives a few microseconds later than the appearance of the second peak; (2) it is well known that cylindrical wave propagation is accompanied by a $1/\sqrt{x}$ type decay in amplitude.

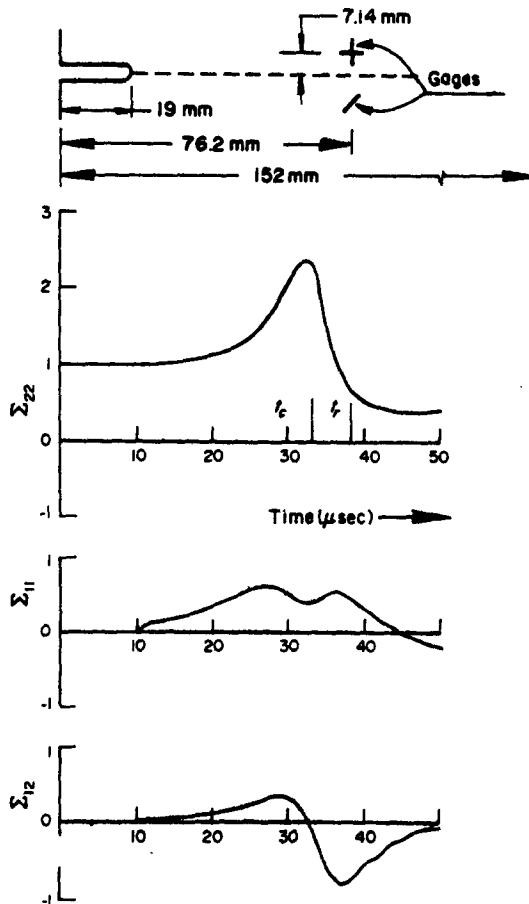


Fig. 4. Dynamic stresses produced by the fracture of the specimen shown.

Now the waves emitted by the crack tip undergo a cylindrical expansion, suffer a reflection at the right edge, and then begin to arrive at the gage location at $t = 38.4 \mu\text{sec}$. The distance traveled by the front (210 mm) is much larger than the characteristic dimensions associated with the crack propagation. Therefore, it is most unlikely that any significant amount of *energy* arrives with the arrival of the wavefront. Nevertheless, we would like to emphasize that the data is not strictly valid for $t > t_r = 38.4 \mu\text{sec}$.

The next test was conducted with the same x_1 location of the strain gages but with $x_2 = 19 \text{ mm}$ (0.75 in) instead of 7.14 mm as in Fig. 4; the objective was to study the influence of x_2 on the shapes of emitted pulses. Results of a typical test are shown in Fig. 5. In view of the small change in x_2/x_1 , from 0.111 in Fig. 4 to 0.333 in Fig. 5 the pulse shapes are remarkably different for the two cases. The peak in Σ_{22} is much smaller, and the trace is characterized by relatively smaller gradients. Unfortunately, analytical solution for dynamic stresses at a point away from the crack path are not yet available. Figures 4 and 5 have been included here for the sake of comparison with the theoretical results as and when they become available.

Finally, as was discussed in the Introduction, Kinra and Kolsky in their work with fracture of beams in *pure bending*[4] observed that the passage of the crack-tip from the initially tensile to the initially compressive half of the beam is *not* accompanied by any appreciable changes in crack speed. Our results in Figs. 3-5 show that the stress field radiated in front of the tip is tensile in all in-plane directions and thereby provides a mechanism by which the foregoing is made possible.

CONCLUSIONS

The dynamic stress field in the vicinity of the crack plane when single-edge-notched plates of soda-lime glass are subjected to brittle fracture in pure tension has been examined in detail.

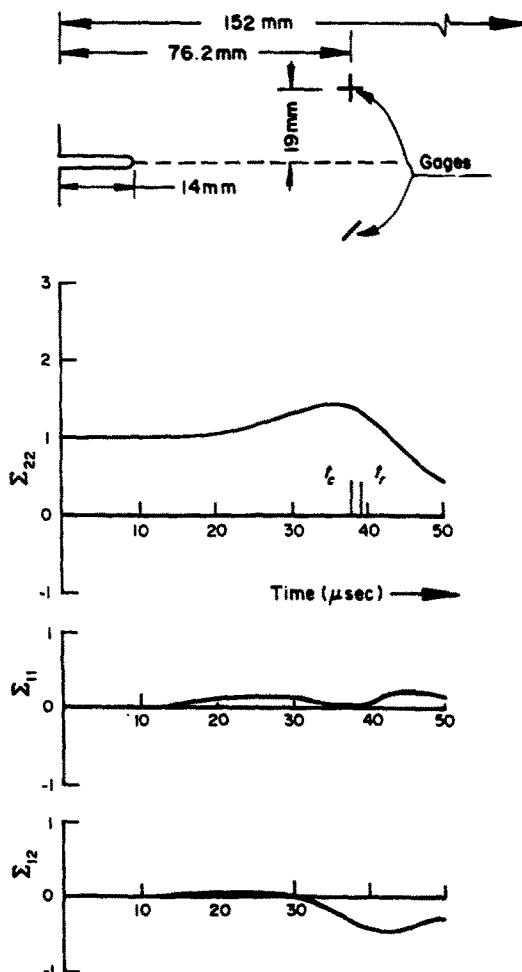


Fig. 5. Dynamic stresses produced by the fracture of the specimen shown.

For the case of points lying on the prospective fracture path, it was found that both the radial and the circumferential stresses are tensile and that the experimental results are in good agreement with the predictions of an earlier work due to Freund, in spite of the fact that the analysis is based on plane strain assumption, while the experiments were carried out in plane stress conditions. Experimental results for points not lying on the fracture plane have been reported for comparison with the corresponding analytical work as and when it becomes available.

Acknowledgements—The authors wish to express their sincere appreciation to Profs. W. E. Jahsman and S. K. Datta for many helpful discussions. Thanks are due to Karl Rupp, Edward McKenna and Charles Coet for their technical assistance and to Nickie Ashley for a careful preparation of the manuscript. Thanks are also due to Dr. Howard Swift, Director of Research and Development, Libbey-Owens-Ford Company, for supplying the glass specimens.

The financial support of the National Science Foundation under the grant ENG 76-09613 to the University of Colorado is gratefully acknowledged.

REFERENCES

1. L. B. Freund, Dynamic crack propagation. In *The Mechanics of Fracture* (Edited by F. Erdogan), Vol. 19, p. 105. ASME AMD (1976).
2. L. R. F. Rose, Recent theoretical and experimental results on fast brittle fracture. *Int. J. Fracture* **12**(6), 799–813 (1976).
3. V. K. Kinra, Stress pulses emitted during fracture in tension. *Int. J. Solids Structures* **12**, 803–808 (1976).
4. V. K. Kinra and H. Kolsky, The interaction between bending fractures and the emitted stress waves. *Engng Fracture Mech.* **9**, 423–432 (1977).
5. A. S. Kobayashi and S. Mall, Rapid crack propagation and arrest in polymers. Department of Mechanical Engineering, College of Engineering, University of Washington, *Tech. Rep. No. 30* (1977).
6. L. B. Freund, Crack propagation in an elastic solid subjected to general loading—I. Constant rate of extension. *J. Mech. Physics Solids* **20**, 129–140 (1977).
7. L. B. Freund, The initial wave front emitted by a suddenly extending crack in an elastic solid. *J. Appl. Mech. Trans. of ASME, Series E* **39**, 601–602 (1977).
8. R. B. Heywood, *Designing by Photoelasticity*. Chapman & Hall, London (1952).
9. J. R. Rice, Mathematical analysis in the mechanics of fracture. In *Fracture. An Advanced Treatise* (Edited by H. Liebowitz), Vol. II, pp. 191–311. Academic Press, New York (1968).
10. T. L. Paxson and R. A. Lucas, An experimental investigation of the velocity characteristics of a fixed boundary fracture model. In *Dynamic Crack Propagation* (Edited by G. C. Sih). Noordhoff (1973).
11. H. Kolsky, *Stress Waves in Solids*. Dover (1963).